Dynamically integrated transport approach for high-energy nuclear collisions at high baryon density

Koichi Murase (Sophia University)

based on Phys. Rev. C98, 024909 (2018) [arXiv:1805.09024 [nucl-th]]

Collaboration with
Yukinao Akamatsu, Masayuki Asakawa (Osaka University)
Tetsufumi Hirano (Sophia University)
Masakiyo Kitazawa (Osaka University, KEK, J-PARC)
Kenji Morita (QST, University of Wroclaw, RNC)
Yasushi Nara (Akita International University)
Chiho Nonaka (Nagoya University, KMI)
Akira Ohnishi (Kyoto University)

The 8th International Conference on Quarks and Nuclear Physics (QNP2018)

Nov 16, 2018, Tsukuba, Japan

Introduction

QCD critical point/1st-order phase transition search

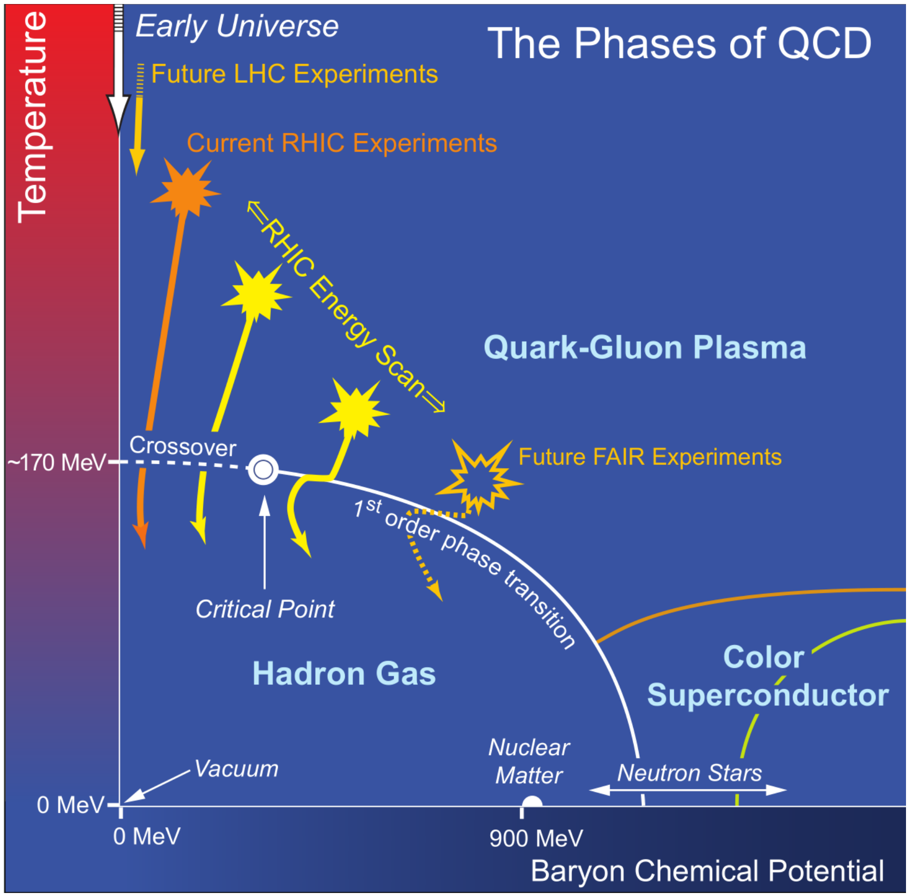

Schematic phase diagram of QCD
[taken from the 2007 NSAC Long Range Plan]

Beam energy scan for high-energy heavy-ion collisions

Search high-baryon density domain of phase diagram in RHIC, SPS, FAIR, NICA, J-PARC, etc.

MODEL

Dynamical modeling

Transport models (such as *hydro model* and *microscopic transport model*)
needed to extract *physical information of created matter* from *final hadron spectra*

Three important notions in lower energy collisions
(which are closely related to one another)

- **Dynamical initialization**:
  hydrodynamics initialized via *source terms*
- **Dynamical core-corona separation**:
  thermalized region (*core*) and other part (*corona*)
- **Dynamical integration**:
  microscopic transport model and hydro dynamically coupled to each other

Dynamical initialization

High-energy collisions at RHIC/LHC

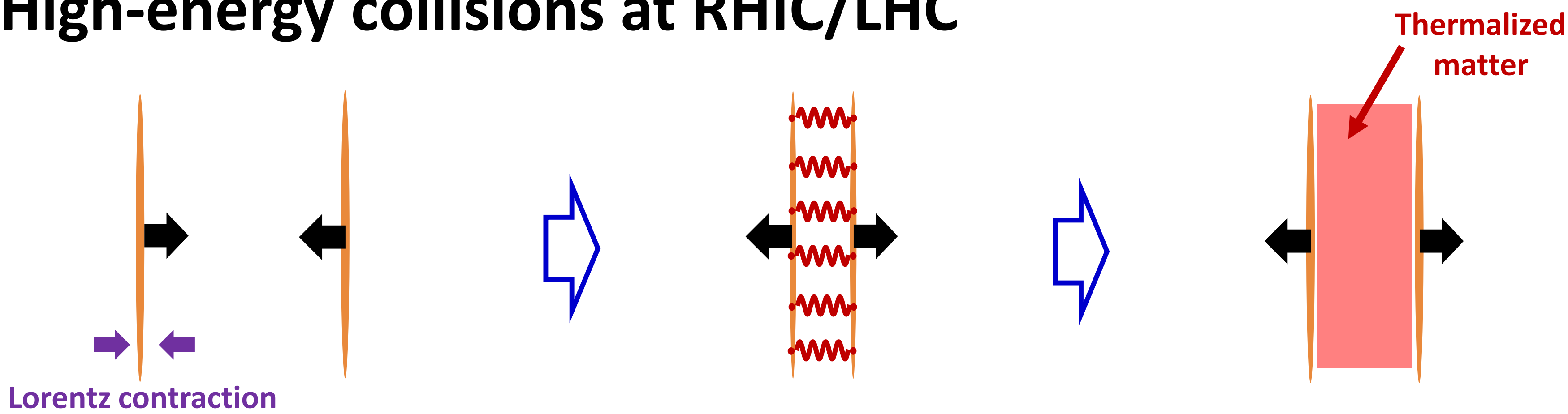

Lower-energy collisions

detailed description required

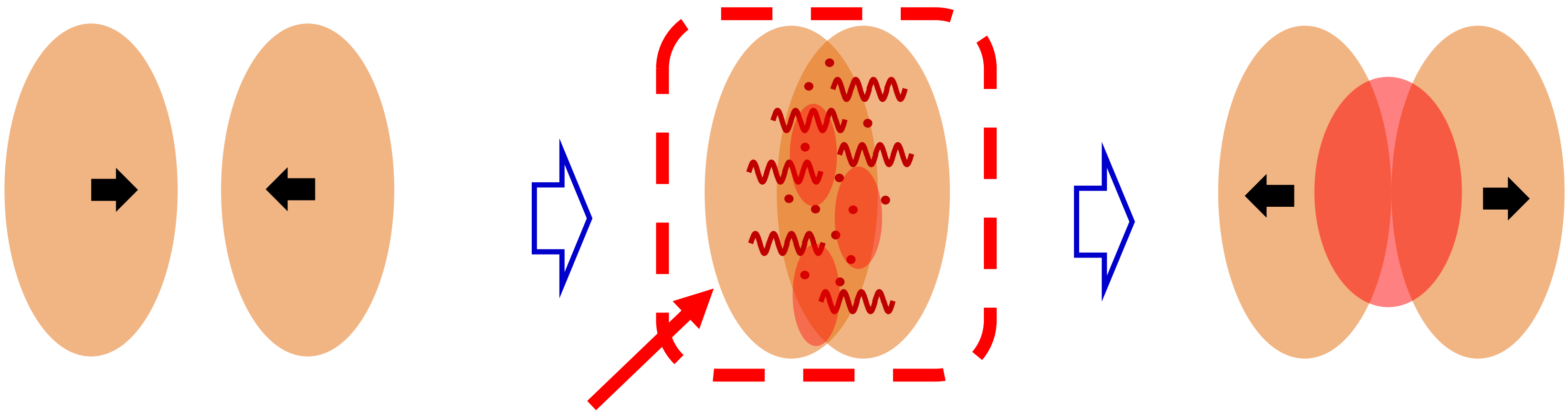

dynamical description of this non-equilibrium process

= <u>Dynamical initialization</u>

Okai, Kawaguchi, Tachibana, Hirano, PRC95, 054914 (2017); C. Shen, B. Schenke, PRC, 024907 (2018)

Dynamical core-corona separation

Fixed-time conversion to hydro

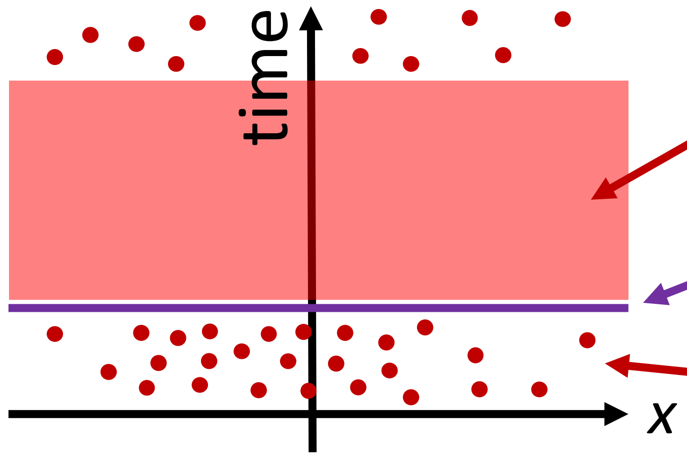

Thermalized matter
described by hydrodynamics

Fixed switching time

Non-equilibrium state
described by microscopic models

Core-corona separation in space and time

K. Werner, PRL98, 152301 (2007)
C. Shen, B. Schenke, PRC97, 024907 (2018)

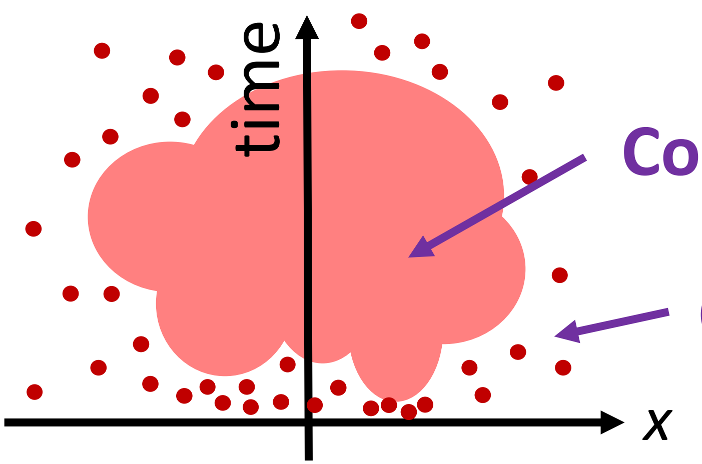

Core = Thermalized spacetime region
described by hydrodynamics

Corona = Unthermalized spacetime region
described by microscopic models

Dynamical integration

Conventional integration of hydro & cascades

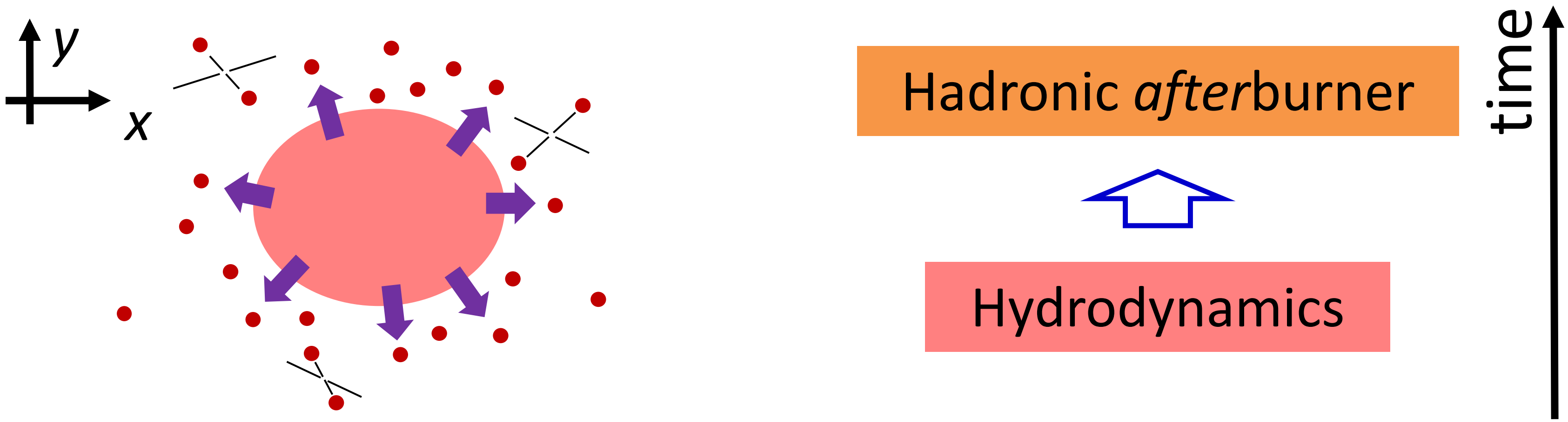

Dynamical integration

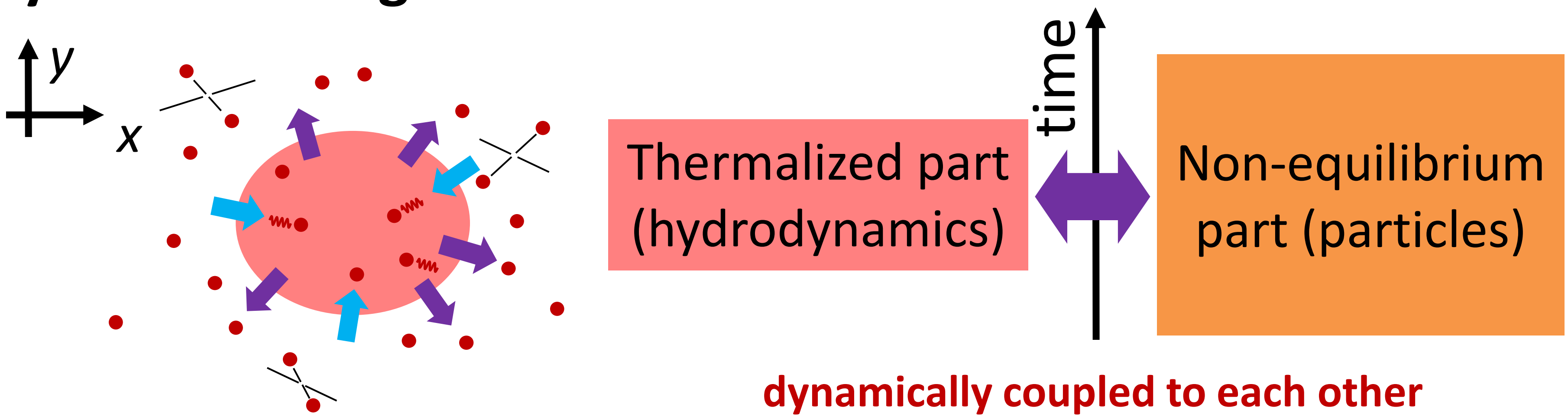

dynamically coupled to each other

JAM+hydro model (JAM 1.9)

JAM cascade

Binary collisions of particles

String excitation:
same scheme with HIJING

String fragmentation:
PYTHIA6 Lund model

Resonance decays

Core

$e > e_f$

Decay
Fragmentation

e_f = 0.5--1.0 GeV/fm^3

$e < e_p$

Cooper-Frye formula

e_p = 0.5 GeV/fm^3

Ideal hydrodynamics with source terms

$$\partial_\mu T_f^{\mu\nu} = J^\nu$$ Energy momentum

$$\partial_\mu N_f^{\mu} = \rho$$ Baryon currents

HLLE scheme
with modified MC limiter

var Leer, J. Comput, Phys. 32, 101 (1979)
K. Okamoto, C. Nonaka, Eur. Phys. J. C77, 383 (2017)

EOS-Q: Sollfrank, Huovinen, Kataja, Ruuskanen, Prakash, Venugopalan, PRC55, 392 (1997)
Kolb, Sollfrank, Heinz, PLB459, 667 (1999(, PRC62, 054909 (2000)

phenomenological EoS with
1st order phase transition
$B^{1/4}$ = 235 GeV/fm^3
$V(\rho_B) = K\rho_B$ in hadron phase

RESULTS

Evolution of particles/hydro energies

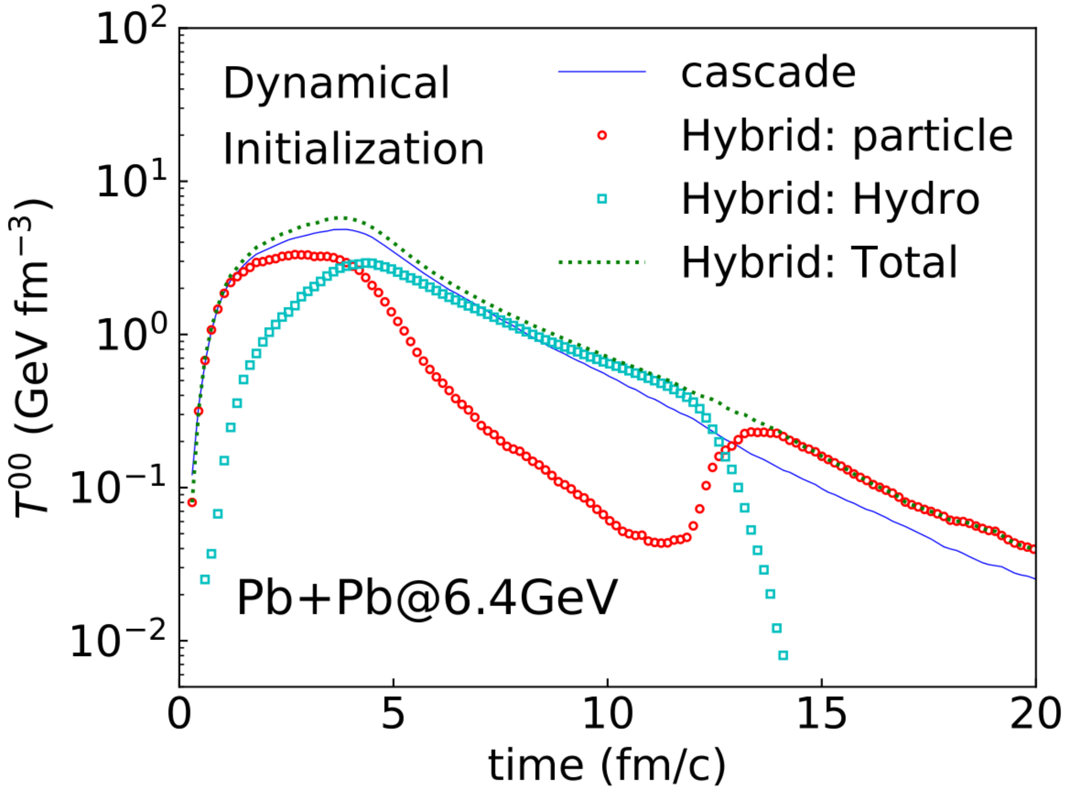

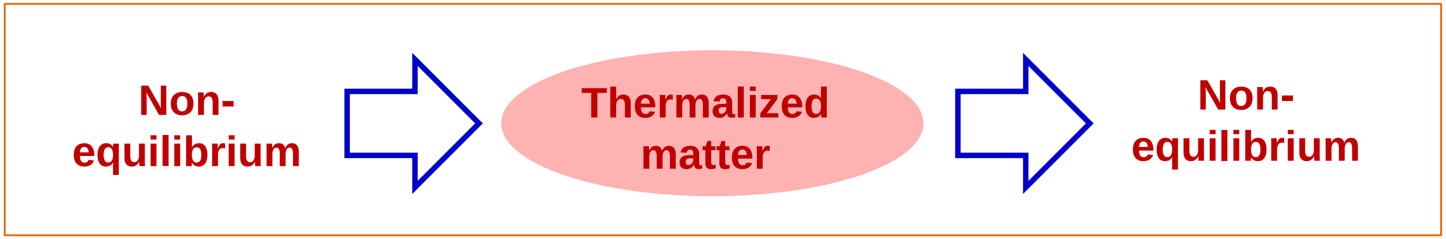

Slower expansion compared to JAM cascade w/o hydro

Phys. Rev. C98, 024909 (2018) [arXiv:1805.09024 [nucl-th]]

Fluid fraction of different energies

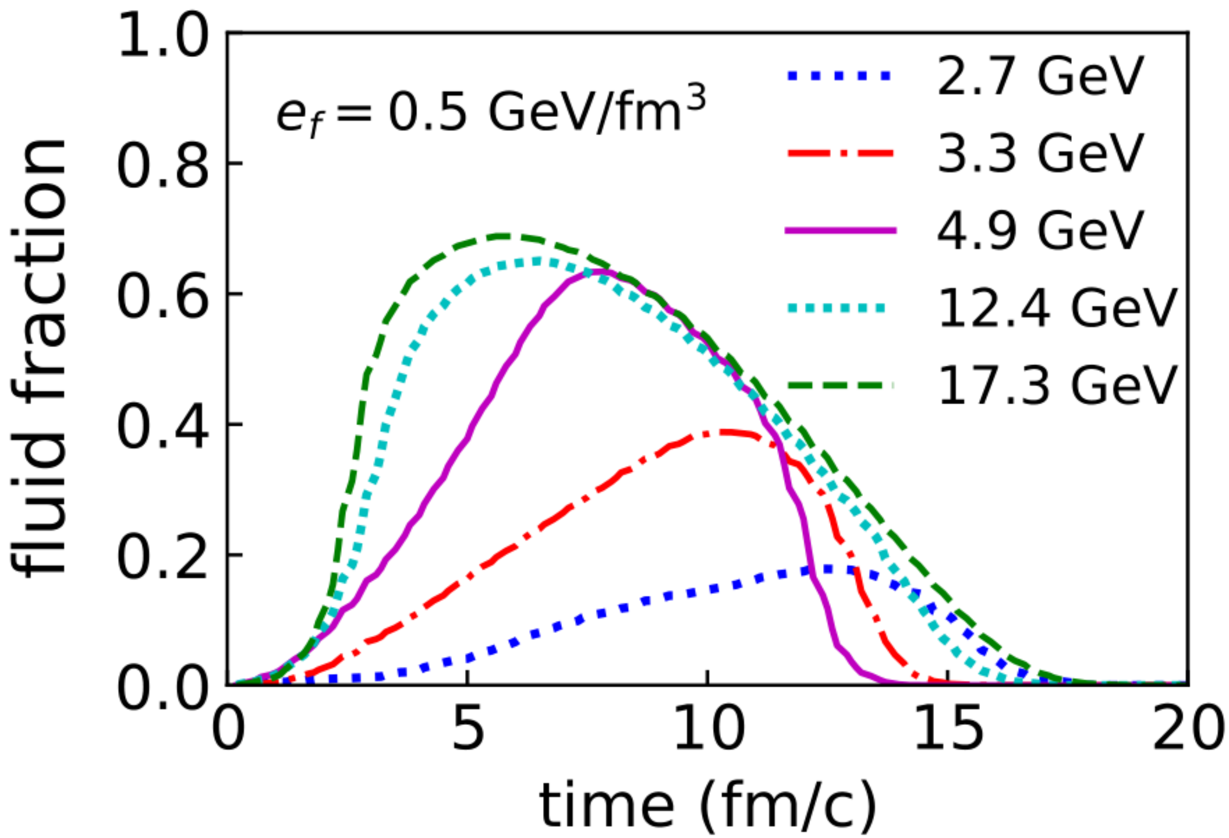

Lower energies
Particle fraction large

Energy $\sqrt{s_{NN}}$

Higher energies
Fluid fraction large
→ fixed-time init

Phys. Rev. C98, 024909 (2018) [arXiv:1805.09024 [nucl-th]]

dN/dy for $p/\pi/K/\Lambda+\Sigma^0$

Pb+Pb 6.4 GeV Central 0-7%

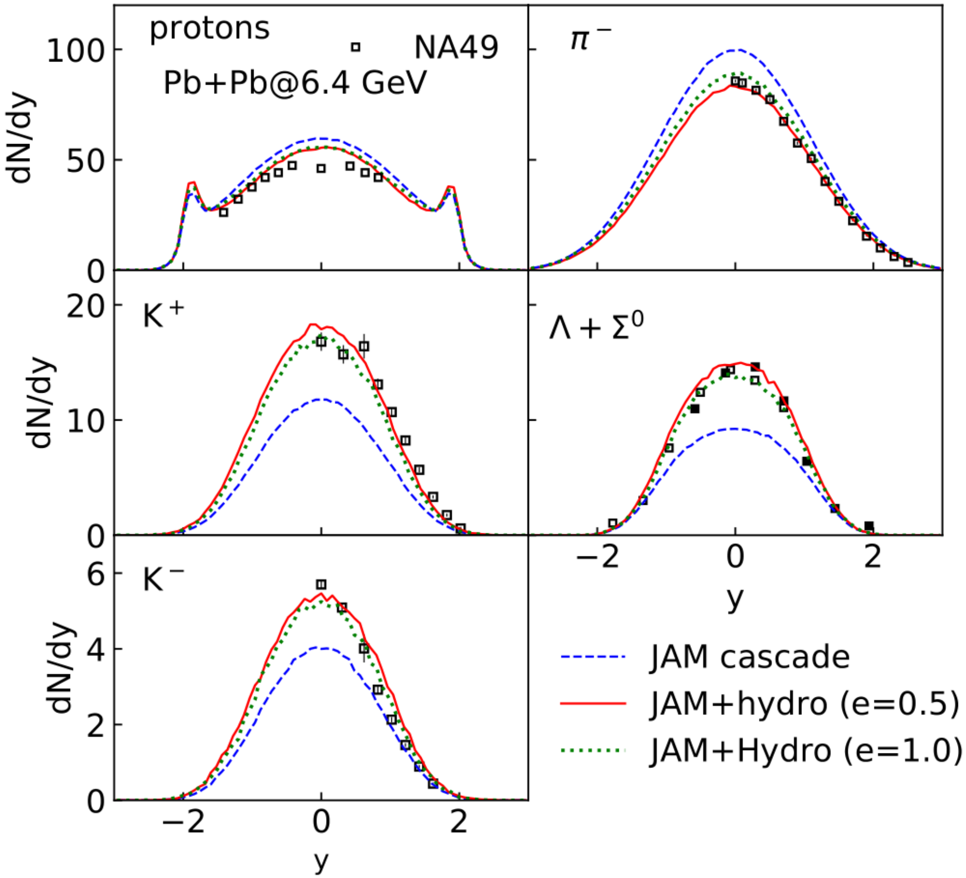

data: NA49, J. Phys. G 34, S951 (2007); NA49, PRC77, 024903 (2008); NA49, PRC78, 034918 (2008)

Compared to JAM cascade w/o hydro…

Protons almost the same
= Similar stopping power
Note: leading hadrons not converted into hydro

Decrease of pions,
Increase of strange hadrons
= Strangeness enhancement
← chemical equilibration
← conversion to hydro

Results insensitive to
e_f = 0.5--1.0 GeV/fm^3

dN/dy vs $\sqrt{s_{NN}}$

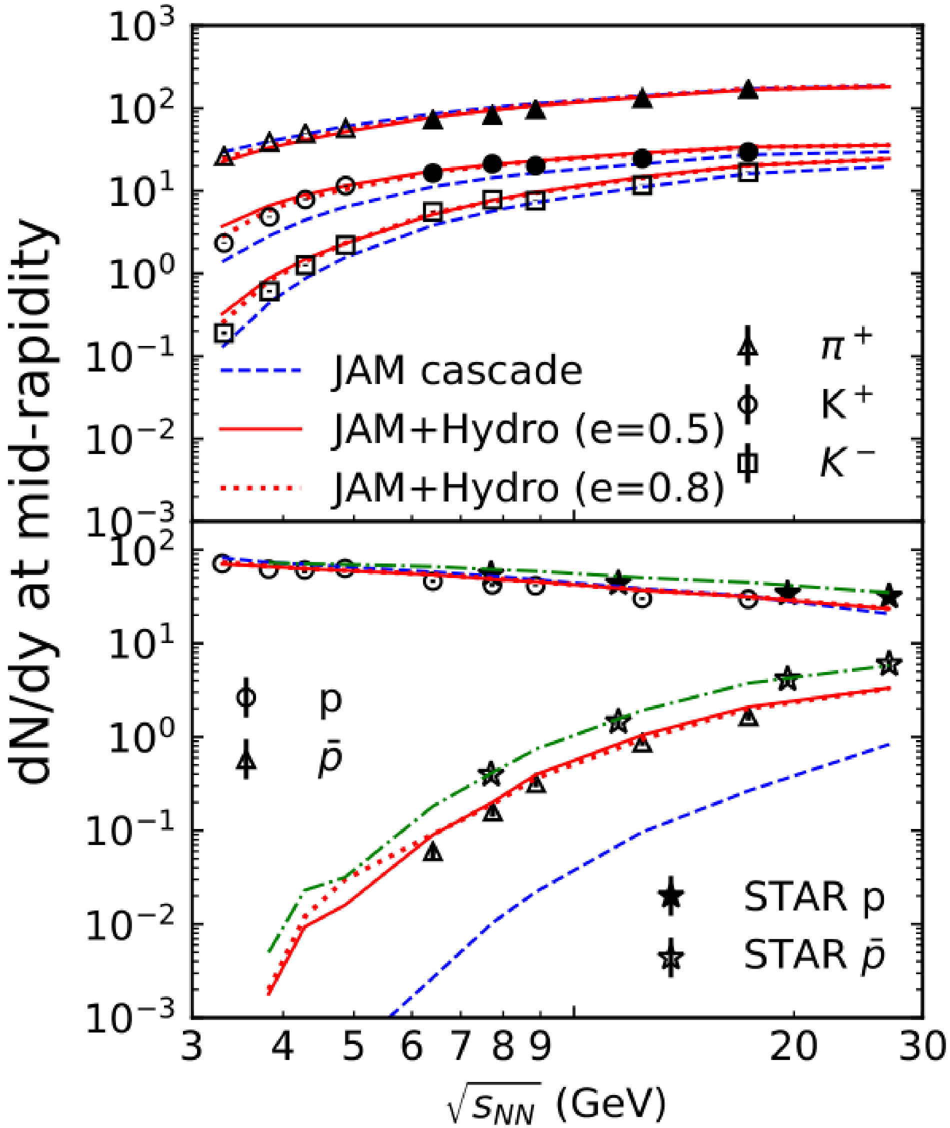

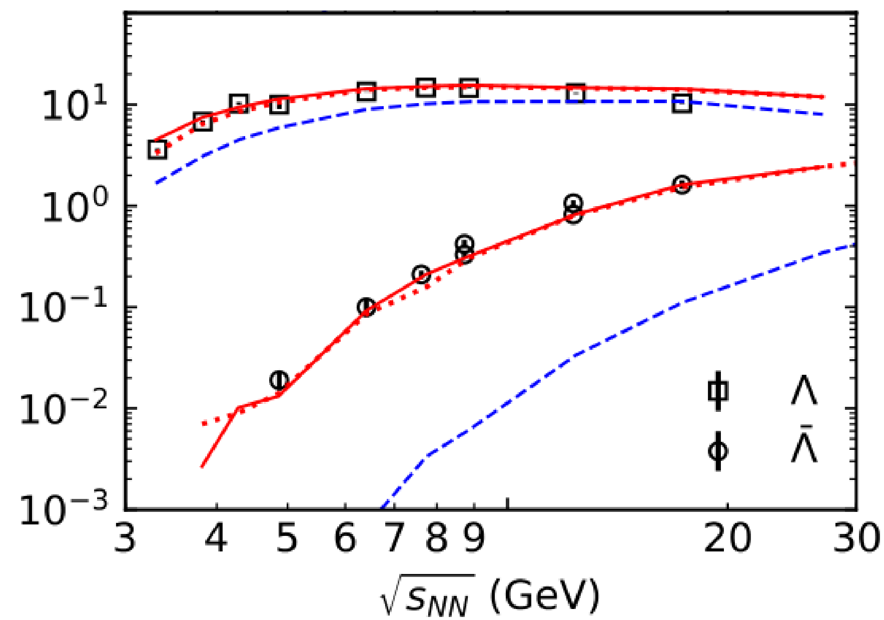

Central Pb+Pb collisions

data: E866 and E917, PLB476, 1 (2000); Blume, Markert, PPNP66, 834 (2011); E802, PRC57, R466 (1998); E895, PRL88, 102301 (2002)

Reproduce
dN/dy energy dependence
for π, K, p, p^{bar}, Λ, Λ^{bar}

Phys. Rev. C98, 024909 (2018) [arXiv:1805.09024 [nucl-th]]

K / π ratio vs $\sqrt{s_{NN}}$

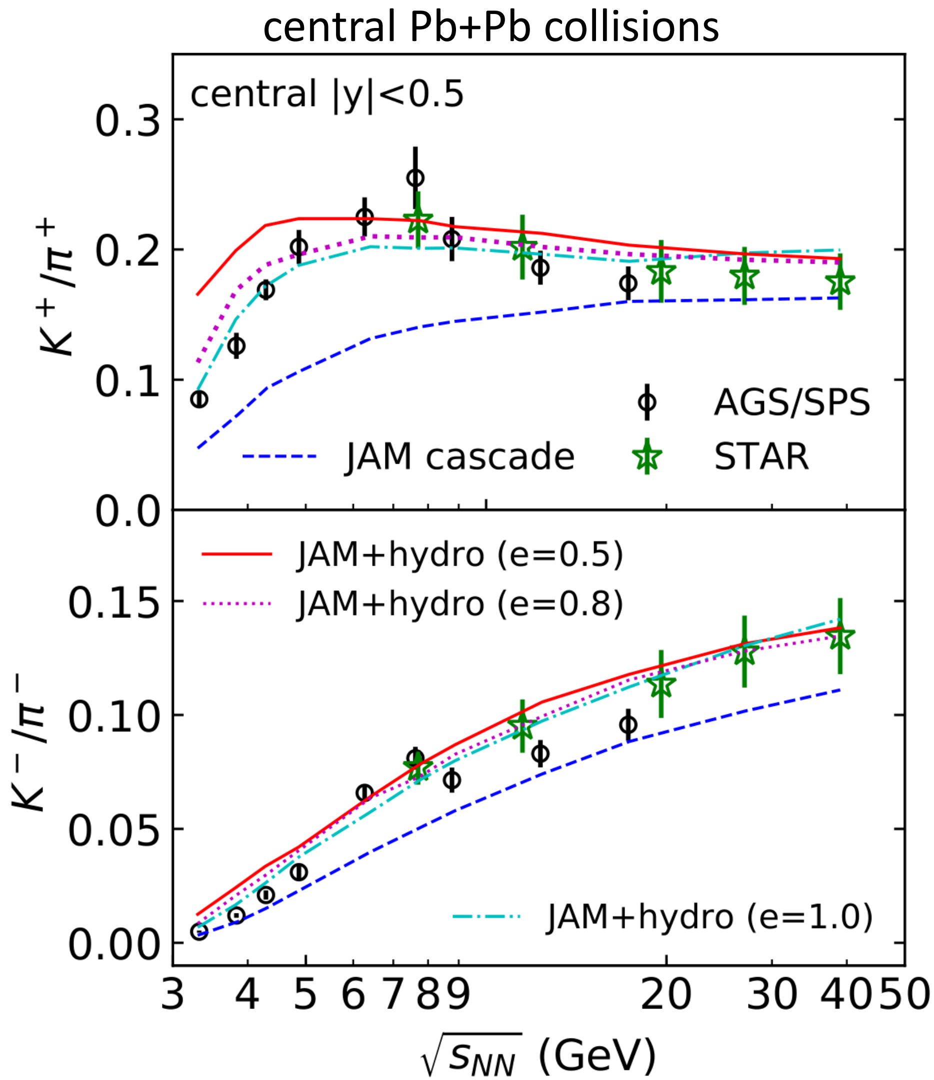

data from NA49, PRC66, 054902 (2002); NA49, PRC77, 024903 (2008); STAR, PRC96, 044904 (2017)

Consistent with experimental "horn"

At lower energies:
Sensitive to e_f. Higher e_f than e_p = 0.5 GeV/fm^3 is favored

At higher energies:
Less sensitive to e_f

Phys. Rev. C98, 024909 (2018) [arXiv:1805.09024 [nucl-th]]

$(\Lambda + \Sigma^0) / \pi^-$ ratio vs $\sqrt{s_{NN}}$

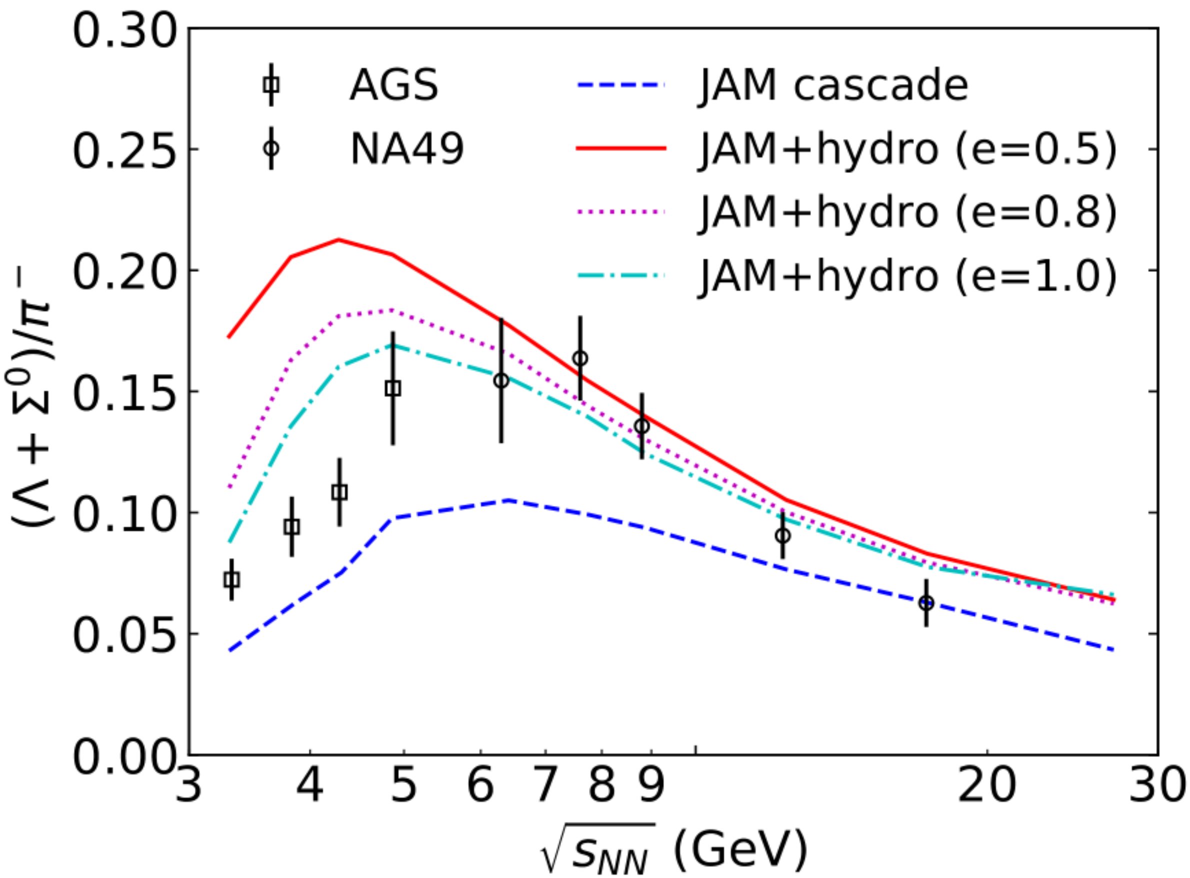

central Pb+Pb collisions

data: NA49, PRL93, 022302 (2004); STAR, PRC83, 024901 (2011)

Describes data well at higher energies.
Overestimates at lower energies.

Phys. Rev. C98, 024909 (2018) [arXiv:1805.09024 [nucl-th]]

SUMMARY

Summary/Outlook

JAM + hydro hybrid model Phys. Rev. C98, 024909 (2018) [arXiv:1805.09024 [nucl-th]]

- Dynamical initialization/core-corona sep./integration
- Reproduce various experimental data
  - Rapidity distribution for $p/\pi/K/\Lambda+\Sigma^0$,
  - dN/dy vs $\sqrt{s_{NN}}$ for $\pi/K/p/p^{bar}/\Lambda/\Lambda^{bar}$,
  - K/π, $(\Lambda+\Sigma^0)/\pi$ ratio vs $\sqrt{s_{NN}}$, etc.

Outlook

- Various observables and centrality dependence: multistrange particles, dv_1/dy, v_2, etc.
- Sensitivity to EoS, viscous effects
- Full particle-fluid interaction: energy deposition of particles traveling through the medium

BACKUP

Particles to Fluid

- Absorption of particles into fluid

Source terms for hydrodynamics

$$J^\mu(\boldsymbol{r}) = \frac{1}{\Delta t} \sum_i p_i^\mu(t) G(\boldsymbol{r} - \boldsymbol{r}_i(t)),$$

$$\rho(\boldsymbol{r}) = \frac{1}{\Delta t} \sum_i B_i G(\boldsymbol{r} - \boldsymbol{r}_i(t)),$$

Lorentz-contracted deposition profile

$$G(\boldsymbol{r}) = \frac{\gamma}{(2\pi\sigma^2)^{3/2}} \exp\left(-\frac{\boldsymbol{r}^2 + (\boldsymbol{r}\cdot\boldsymbol{u})^2}{2\sigma^2}\right),$$

Fluid to particles

- Sample particles by Cooper-Frye formula

Positive contribution of Cooper-Frye formula

$$\Delta N_i = \frac{g_i}{(2\pi)^3} \int \frac{d^3p}{E} \frac{[\Delta\sigma \cdot p]_+}{\exp[(p \cdot u - \mu_i)/T] \pm 1},$$

$$[\cdots]_+ \;=\; \theta(\cdots)|\cdots|$$

Effective baryon chemical potential consistent with EoS

$$\mu_B^{\mathrm{eff}} = \mu_B - V(\rho_B) = \mu_B - K\rho_B$$

Backup: dN/dy comparisons

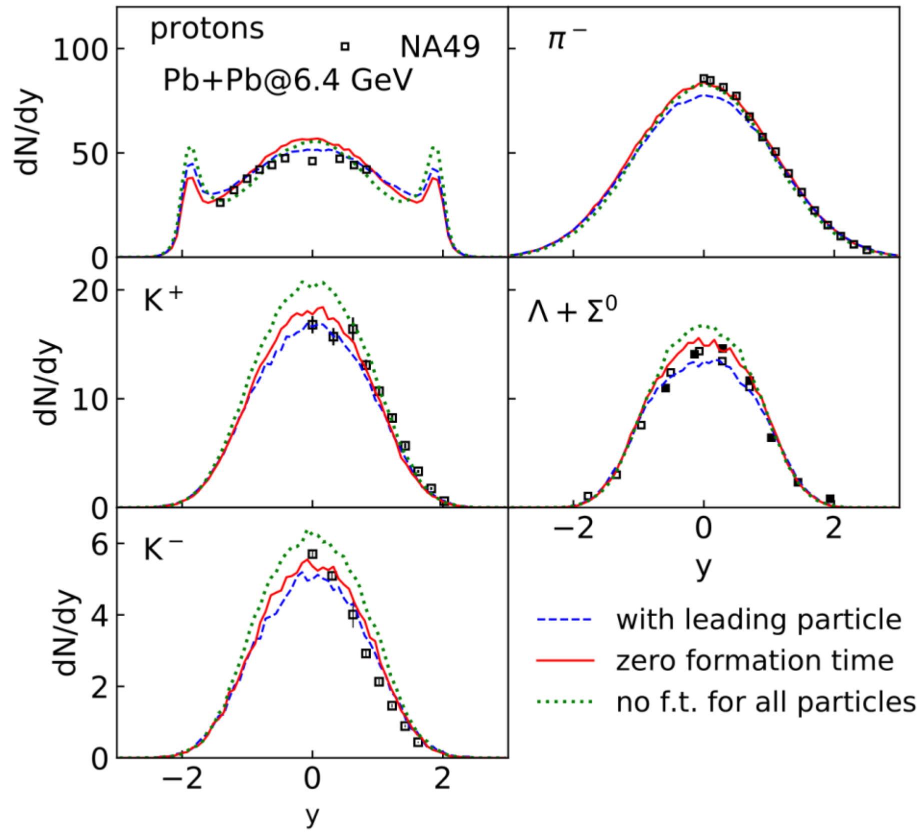

Blue: Stopping power decreased by conversion of leading particles to hydro

Red: effects of formation time negligible

Green: overshoots strange hadron production with everything converted to hydro (equiv. to one-fluid model)

Phys. Rev. C98, 024909 (2018) [arXiv:1805.09024 [nucl-th]]

Backup: m_T distributions

Pb+Pb 6.4 GeV Central 0-5%

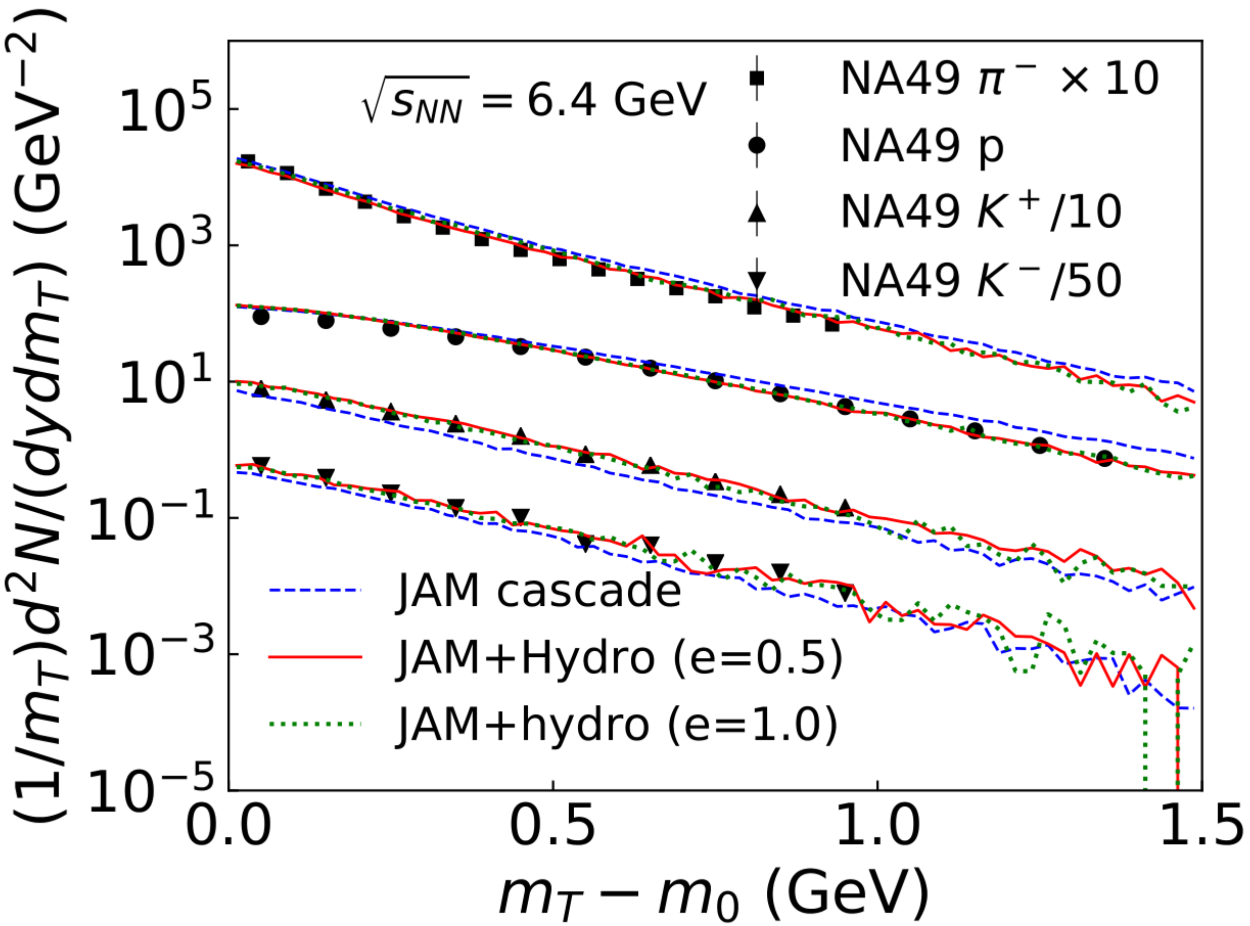

Phys. Rev. C98, 024909 (2018) [arXiv:1805.09024 [nucl-th]]

Backup: $\langle m_T \rangle$ excitation function

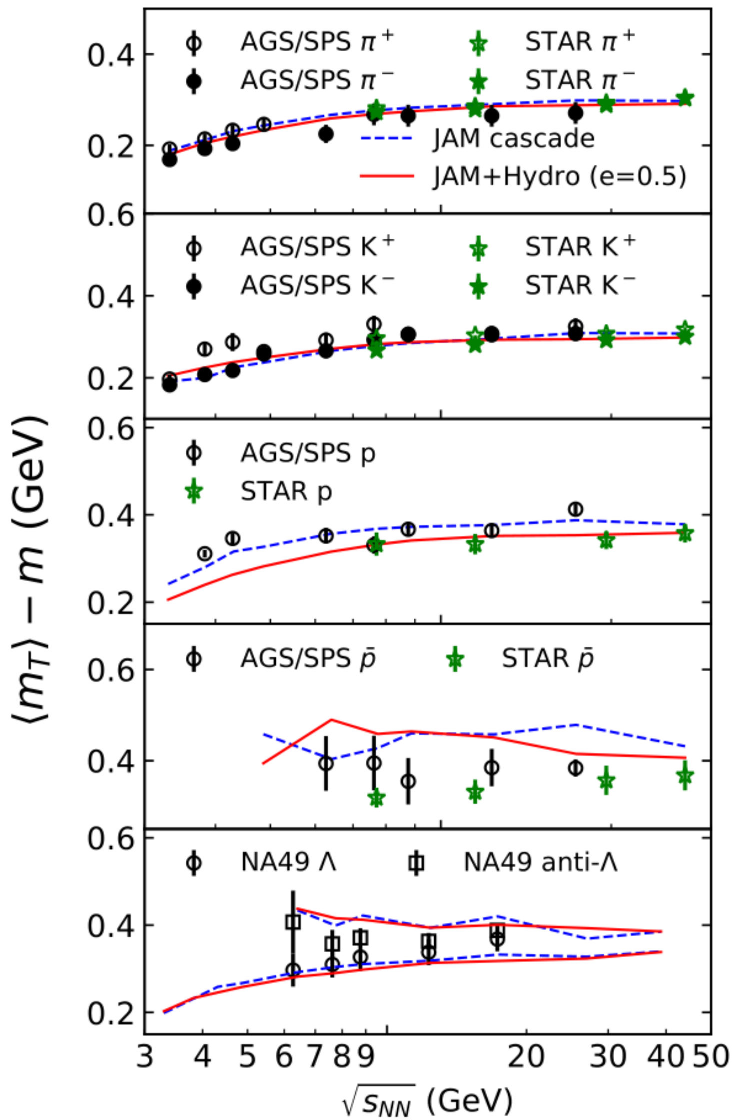

proton: decreased by hydrodynamics

others: unaffected by hydrodynamics

Phys. Rev. C98, 024909 (2018) [arXiv:1805.09024 [nucl-th]]

Backup: Comparison to UrQMD+hydro

Compared to UrQMD+hydro core-corona model
J. Steinheimer and M. Bleicher, PRC84, 024905 (2011)